euspen's 24th International Conference & Exhibition, Dublin, IE, June 2024
www.euspen.eu

Measurement of workpiece deformation based on a sensory chuck

Berend Denkena[1], Heinrich Klemme[1], Eike Wnendt[1]

[1]*Leibniz University Hannover, Institute of Production Engineering and Machine Tools*

wnendt@ifw.uni-hannover.de

Abstract

Achieving tight tolerances is a challenging problem encountered during turning of thin-walled workpieces. Due to the low stiffness of thin-walled workpieces, inadequate workpiece deformation can occur even when clamping forces are low. Therefore, the workpiece deformation needs to be precisely controlled. Conventional approaches use additional measuring devices (e.g. a touch probe) to measure the workpiece deformation. Afterwards, the clamping force is adjusted accordingly in an iterative, manual process step resulting in non-productive time. To ensure low workpiece deformation and reduce non-productive time, a chuck is required which combines workpiece deformation measurement and automatic clamping force adjustment. Thus, this paper presents a novel method to measure workpiece deformation using a chuck with four integrated electric drives. The electric drives are used to precisely adjust the clamping force. Based on the measured clamping force, the workpiece deformation is calculated considering previously identified correlations between the clamping force and the workpiece deformation. To identify these correlations, workpieces with different ratios between inner to outer diameter are clamped and the resulting workpiece deformation is measured using a coordinate measuring machine. The new method allows to measure workpiece deformations within a tight tolerance grad of up to ISO 286 IT5.

Keywords: Sensory chuck, thin-walled workpieces, deformation, precision clamping

1. Introduction

Precision turning of thin-walled workpieces such as bearings, tubes or hollow shafts is of key importance in aerospace, automotive and medical applications [1, 2]. The system to clamp the workpiece has a significant influence on the achievable machining accuracy [3]. To ensure high machining accuracy, clamping systems with special designs, e.g. floating jaws, collet or diaphragm chucks were developed [4, 5]. However, these clamping systems are only suitable for certain workpiece diameters or manufacturing processes. In contrast, the most commonly used clamping device in turning are chucks with three or four jaws [3]. Jaw-chucks allow an adaptable clamping of different workpiece diameters. Therefore, jaw-chucks are universally used for turning. However, the clamping forces of the jaws applied to a thin-walled and thus elastic workpiece lead to shape deformation (Fig. 1) even when clamping forces are low [7].

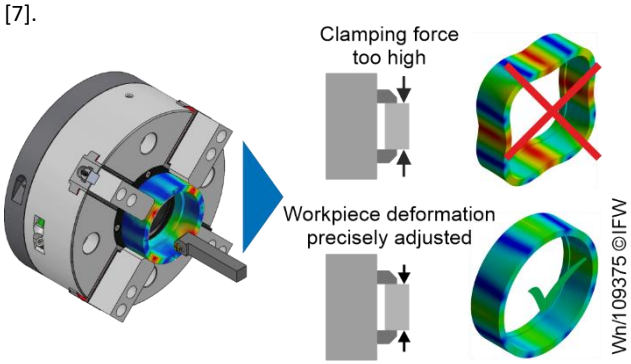

Figure 1. Workpiece deformation caused by clamping force

For jaw-chucks, the workpiece deformation needs to be determined in order to adjust the clamping force if necessary. Conventional approaches measure the workpiece deformation directly by a contact measurement device (e.g. a touch probe or dial test indicator) [8]. In addition, systems for contactless measurement of workpiece deformation have been developed [9-11]. Furthermore, methods to indirectly measure workpiece deformation based on FE-simulations or analytical calculations have been proposed [12]. In this context, Sergeev et al. proposed an algorithm to adjust the appropriate clamping force by an external clamping cylinder [13]. However, due to losses in the force transmission between cylinder and chuck, high clamping force errors and thus shape deviations of 12-15% occur.

In summary, the deformation determination and clamping force adjustment is typically performed manually in an iterative and thus time-consuming process step. For this reason, a novel chuck is presented in this paper, which combines workpiece deformation measurement and automatic clamping force adjustment. The design of the chuck and the concept to measure workpiece deformation are explained in section 2. In section 3, the achievable workpiece deformation measurement accuracy is analysed.

2. Sensory chuck for thin-walled workpieces

In this section, the design of the sensory chuck is described in section 2.1. Afterwards, the concept to measure and control workpiece deformation is explained in section 2.2.

2.1. Sensory chuck design

The design of the sensory chuck is shown in Fig. 2. It is composed of two different modules: A standard four-jaw-chuck VT-S031 from HWR Spanntechnik GmbH and a module with four electrical actuator units. A four-jaw chuck is capable of clamping cylindrical, prismatic as well as irregularly shaped workpieces. This is achieved by a balancing clamping mechanism. The

clamping mechanism ensures that the clamping force F_{cl} is only applied on the workpiece once there is contact on all four clamping jaws. To apply the clamping force, the actuation force F_{act} is required. Therefore, four electrical actuator units are integrated into the chuck. Each of the four actuator units consists of a leadscrew and a FHA-14C gear motor from Harmonic Drive SE. The leadscrew allows the transmission of rotational movement of the motor into a linear positioning movement required to actuate the four-jaw-chuck. The leadscrews are mechanically connected in parallel via a coupling element to transmit the actuating force F_{act}.

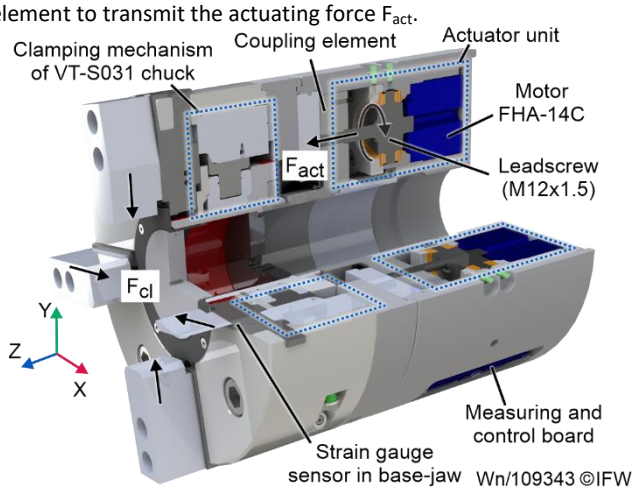

Figure 2. Sensory chuck design

A total of four EJ7411 measuring and control boards from Beckhoff Automation GmbH & Co. KG are integrated into the chuck. Each EJ7411-module can measure and control the drive signals (motor current I_m, angular position p) in a closed feedback loop. Furthermore, a strain gauge sensor of type N2A-06-S1783 from ME-Meßsysteme GmbH is integrated into the base-jaw to measure the clamping force. The EJ7411-modules as well as the strain gauge sensor are part of the measurement and control scheme for workpiece deformation as explained in the following section.

2.2. Concept to measure and control workpiece deformation

The concept to measure workpiece deformation is shown in Fig. 3. The concept is designed for thin-walled, ring-shaped workpieces.

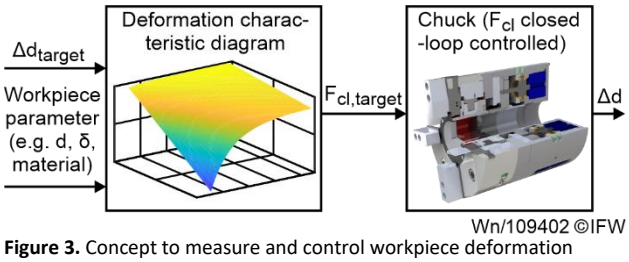

Figure 3. Concept to measure and control workpiece deformation

A linear-elastic workpiece deformation is assumed for the control system. The resulting workpiece deformation Δd correlate therefore linearly proportional to the applied clamping force F_{cl} and the stiffness of the workpiece. The workpiece stiffness is determined by material properties and the geometry of the workpiece. Such workpiece parameters (e.g. workpiece diameter d, diameter ratio δ or material) are provided by the chuck operator and serve as input variables for the deformation characteristic diagram. Based on a provided workpiece deformation tolerance Δd_{target}, the appropriate clamping force is calculated by the deformation characteristic diagram. The calculated clamping force $F_{cl,target}$ is then applied by the chuck in a closed-loop control. The system to measure and control the clamping force does already exist. As described in [14], a low clamping force error of ΔF_{cl} = 1.4% was achieved. In section 3, the deformation characteristic diagram is characterised.

3. Experimental setup and results

In this section, the experimental setup to obtain the deformation characteristic diagram is described in section 3.1. Afterwards, the results are discussed in section 3.2. In this paper, only the influence of geometry parameters on the characteristic diagram is investigated. The experiments were carried out for a total of nine workpiece samples made from the constant material 16MnCr5. Each workpiece sample represents a hollow cylinder with a cylinder height h_Z = 60 mm. The outer diameter d_o is varied between 80 mm and 120 mm, which is a typical workpiece diameter range for the chuck. The other geometry parameters are listed in Table 1. With the selected geometry parameters, the influence of varying geometry parameters (outer diameter d_o, inner diameter d_i, wall thickness s and diameter ratio δ) on the workpiece deformation measurement is analysed in the following chapters.

Table 1 Geometry parameters of the nine workpiece samples

No.	d_o	d_i	$s = (d_o-d_i)/2$	$\delta = d_o/d_i$
1	80 mm	52 mm	14 mm	1,53
2	80 mm	60 mm	10 mm	1,33
3	80 mm	64 mm	8 mm	1,25
4	100 mm	72 mm	14 mm	1,38
5	100 mm	80 mm	10 mm	1,25
6	100 mm	84 mm	8 mm	1,19
7	120 mm	92 mm	14 mm	1,30
8	120 mm	100 mm	10 mm	1,20
9	120 mm	104 mm	8 mm	1,15

3.1. Experimental setup to measure workpiece deformation

The experimental setup is shown in Fig. 4. A coordinate measuring machine was used to determine the contour of the inner surface along the Z-axis on the four clamping jaws.

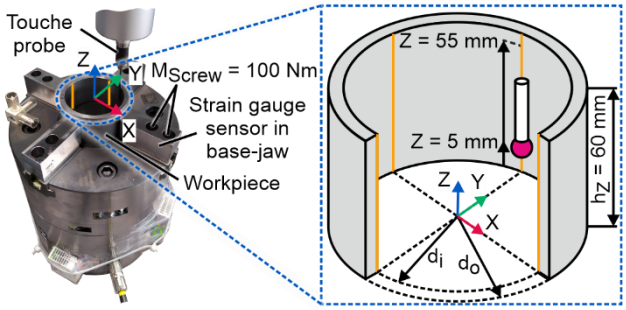

Parameter
Workpiece material 16MnCr5 — Inner diameter d_i = 54 ... 104 mm
Touche probe Leitz X5HD-S — Outer diameter d_o = 80 ... 120 mm
Coordinate measuring machine Leitz Reference XI

Wn/109403 ©IFW

Figure 4. Experimental setup to determine the deformation characteristic diagram

The workpiece contour along the four clamping jaws was measured with five repetitions. This process was repeated for ten clamping force steps (between minimum and maximum clamping force). In the first step, each workpiece sample was clamped with a minimal clamping force $F_{cl,min} \approx 250$ N. Up to the minimum clamping force, a rigid body displacement of the workpiece can occur due to movements of the clamping mechanism. The position of the workpiece can be assumed to be constant above the minimum clamping force. In addition, all nine workpieces are deformed by Δd < 1 µm at the minimum clamping force and therefore below the measuring accuracy of the coordinate measuring machine. The workpiece shape at the minimum clamping force is therefore used as an almost

undeformed reference state. The workpiece deformation is the difference between the inner surface area in the reference state and the inner surface area for the respective clamping force step.

3.2. Deformation characteristic diagram

The workpiece deformation measured along the four clamping jaws is shown as an example for workpiece sample 3 in Fig. 5. For each jaw, the workpiece deformation Δd is shown as the mean value from five measurements for a clamping force F_{cl} = 74 kN.

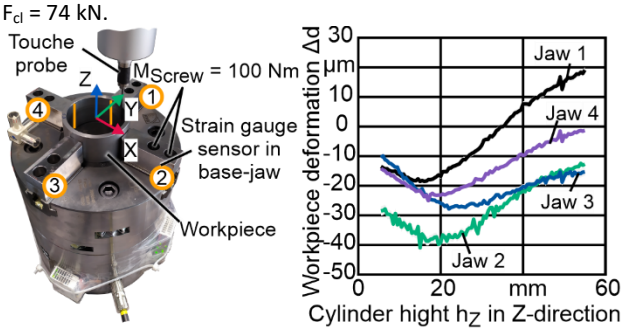

Parameter
Workpiece material 16MnCr5 Inner diameter d_i = 64 mm
Touche probe Leitz X5HD-S Outer diameter d_o = 80 mm
Coordinate measuring machine Leitz Reference XI Wn/109404©IFW

Figure 5. Workpiece deformation of sample 3

The workpiece deformation varies depending on the clamping jaw. This is due to an uneven force distribution on the for four clamping jaws. In contrast, uniform deformation curves are achieved for the sum of the deformation on the opposing clamping jaws. The deformation sum for jaw 1 and jaw 3 is the workpiece deformation Δd_Y and the workpiece deformation Δd_X is the sum of jaw 2 and jaw 4. In Fig 6., the workpiece deformation in X-direction is shown. The curves for both the Y-direction and the other workpiece samples show a similar behaviour.

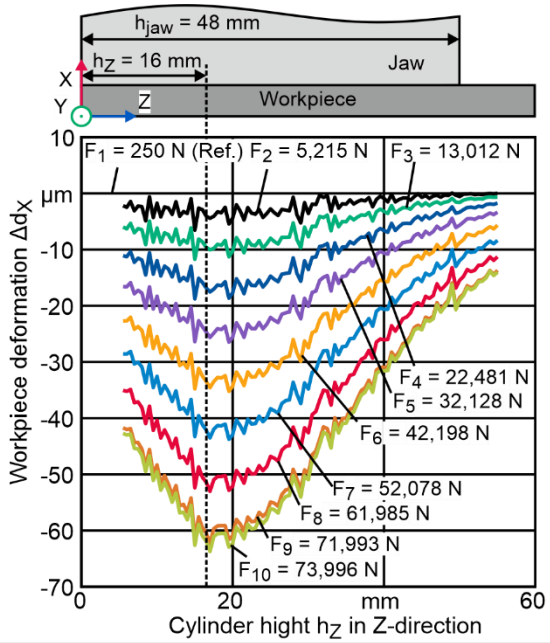

Parameter
Workpiece material 16MnCr5 Inner diameter d_i = 64 mm
Touche probe Leitz X5HD-S Outer diameter d_o = 80 mm
Coordinate measuring machine Leitz Reference XI Wn/109405©IFW

Figure 6. Workpiece deformation for sample 3 in X-direction

Due to the workpiece roughness, deformation peaks occur for every clamping force step at stochastically distributed cylinder heights. In addition, the deformation along the cylinder height occurs unevenly. This is due to the application point of the clamping force, which is located at 1/3 of the total clamping jaw height h_{jaw} = 48 mm [15]. This corresponds to a cylinder height h_Z = 16 mm, at which the maximum deformation nearly occurs in both X and Y direction. The deformation maximum is key for the achievable manufacturing accuracy. The deformation maxima are therefore used for the deformation characteristic diagram. In addition, a single deformation characteristic diagram is needed for the proposed deformation control concept. Therefore, the deformation is combined as the mean value of the X and Y directions. The combined deformation maxima for all nine workpiece samples are shown for the clamping force $F_{cl,max}$ = 80 kN in Fig. 7. At a constant clamping force, there is a reciprocal correlation between the diameter ratio of the workpiece samples and the workpiece deformation. For the asymptote δ = 1 (infinite compliance of the workpiece), an infinitely high deformation occurs. For the asymptote δ = ∞ (infinite stiffness of the workpiece), only the chuck is deflected by Δd = 17 µm.

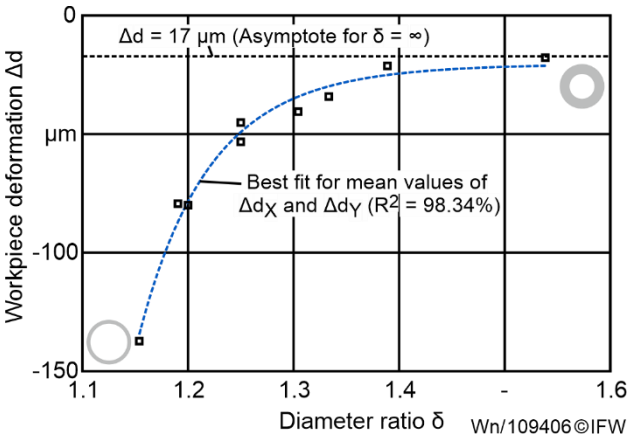

Figure 7. Correlation between diameter ratio and workpiece deformation for $F_{cl,max}$ = 80 kN

If the clamping force is varied (Fig. 8), a linear proportional correlation between the clamping force and the workpiece deformation can be observed.

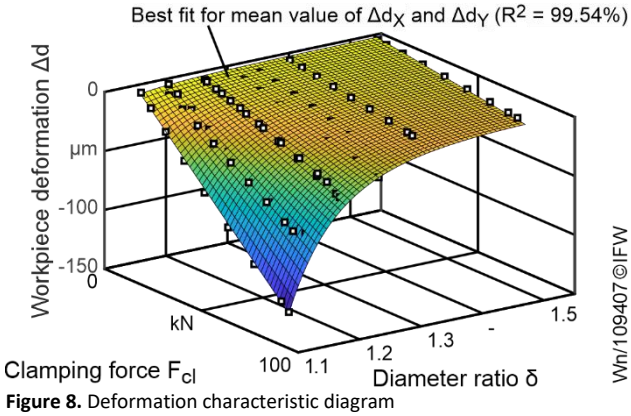

Figure 8. Deformation characteristic diagram

A low standard deviation occurs for each data point with a mean value of σ = 0.65 µm. The chuck can therefore achieve a very high repeatability. In addition, both the linear and the reciprocal correlation between the clamping force F_{cl}, the diameter ratio δ and the resulting workpiece deformation Δd can be approximated by equation (1).

$$\Delta d = (a + b \cdot F_{cl}) \cdot (c \cdot \delta^n + \delta)^2 \quad (1)$$

a = -0.1858; b = -0.07932; c = 12.91; n = -9.109

Equation (1) approximates the deformation characteristic diagram with a high coefficient of determination of R^2 = 99.54%. To evaluate the accuracy of the deformation characteristic diagram, the difference between the characteristic diagram and the measured workpiece deformation was calculated (Fig. 9).

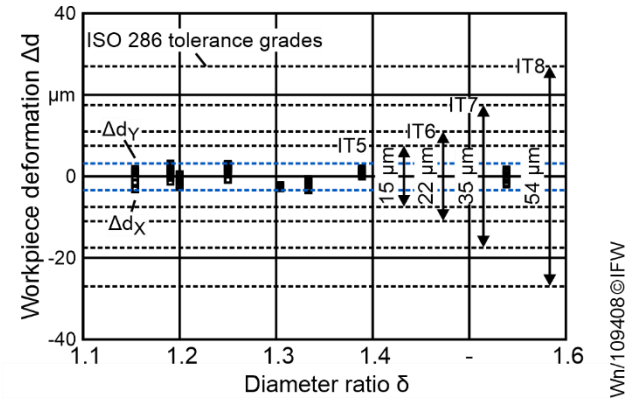

Figure 9. Accuracy of the deformation characteristic diagram

Overall, the characteristic diagram shows a deviation in the range of -3.4 µm to +3.16 µm to the measured deformations. In addition, typical target tolerances for turning according to ISO 286 are shown. The deviations are within a tolerance grade of IT5, which is a commonly used tolerance for precise turning. Consequently, the method for workpiece deformation measurement allows a precise measurement of workpiece deformation. However, the following possible influencing factors on the deformation characteristic diagram must be mentioned:

- The measurements were carried out while the chuck was at a standstill. According to [15], the clamping force varies significantly due to centrifugal forces during turning. Such influence has not yet been quantified.
- In Fig. 5, the deformations on the individual clamping jaws are uneven. This indicates a workpiece tilting due to an alignment error caused by the clamping mechanism. Alignment errors are minimized by jaw boring [16]. However, jaw boring was not performed to maintain identical jaws and thus a constant chuck stiffness.
- Concentricity errors of the workpiece samples occur of up to 194 µm. The influence of shape errors on the deformation characteristic diagram has not yet been quantified.
- An error of up to 2.5 kN occurs when measuring the clamping force with the integrated strain gauge sensor.

4. Conclusion

This paper presents a novel sensing chuck for determining workpiece deformation. The workpiece deformation is calculated considering previously identified correlations between the clamping force and the workpiece deformation. This correlation is approximated by a deformation characteristic diagram with a high coefficient of determination of R^2 = 99.54%. The measurement deviations are within a tolerance grade of ISO 286 IT5, which is a commonly used tolerance for precise turning. Thus, future work aims to evaluate the machining tolerance achieved in cutting processes. In addition, further possible influences on the chuck accuracy (e.g. workpiece misalignment, centrifugal forces during turning) will be investigated.

Acknowledgements

The results presented were obtained within research project “DefCon” (KK5032720JN2). The authors thank the Federal Ministry for Economic Affairs and Climate Action for funding this project as part of the “Central Innovation Program for small and medium-sized enterprises (ZIM)”.

References

[1] Brinksmeier E, Sölter J, Grote C 2007 Distortion engineering – identification of causes for dimensional and form deviations of bearing rings *CIRP Ann.* **56**(1) 109-112
[2] Viitala R 2020 Minimizing the bearing inner ring roundness error with installation shaft 3D grinding to reduce rotor subcritical response *CIRP J. of Manuf. Sci a. Tech.* **30** 140-148
[3] Fleischer J, Denkena B, Winfough B, Mori M 2006 Workpiece and tool handling in metal cutting machines *CIRP Ann.* **55**(2) 817-839
[4] Denkena B, Hülsemeyer L 2015 Investigation of a fine positioning method in lathes using an active clamping chuck *Euspen’s 15th Int. Conf. & Exh.* 245-246
[5] Khaghani A, Cheng K 2020 Investigation on an innovative approach for clamping contact lens mould inserts in ultraprecision machining using an adaptive precision chuck and its application perspectives *Int. J. Adv. Manuf. Tech.* **111** 839-850
[6] Karpuschweski B, Byrne G, Denkena B, Oliveira J, Vereschaka A 2021 Machining Processes *Springer Handb. of Mech. Eng.* 409-460
[7] Estrems M, Carrero-Blanco J, Cumbicus W E, de Francisco O, Sánchez H T 2017 Contact mechanics applied to the machining of thin rings *Proc. Manuf.* **13** 655-662
[8] Valiño G., Suárez C M, Rico J C, Alvarez B J, Blanco B 2012 Comparison between a laser micrometer and a touch trigger probe for workpiece measurement on a CNC lathe *Adv. Mater. Res.* **498** 49-54
[9] Che J K, Ratnam M M 2020 Real-time monitoring of workpiece diameter during turning by vision method *Measurement* **126** 369-377
[10] Fan K C, Chao Y H 1991 In-process dimensional control of the workpiece during turning *Prec. Eng*. **13** (1) 27-32
[11] Kuschmierz R, Davids A, Metschke S, Löffler F, Bosse H, Czarske J, Fischer A 2016 Optical, in situ, three-dimensional, absolute shape measurements in CNC metal working lathes *Int. J. of Adv. Manuf. Tech.* **84** 2739-2749
[12] Manikandan H, Chandra Bera T 2021 Modelling of dimensional and geometric error prediction in turning of thin-walled components. *Prec. Eng*. **72** 382-396
[13] Sergeev A S, Tikhonova Z S, Krainev D V 2017 Automated thrust force calculation of machine tool actuators in fastening and turning steels *Proc. Eng.* **206** 1148-1154
[14] Denkena B, Klemme H, Wnendt E, Meier M 2022 Sensing chuck for thin-walled workpieces *19th Int. Conf. on Prec. Eng.*
[15] Association of German Engineers (VDI) 2004 VDI 3106 – Determination of permissible speed (rpm) of lathe chucks (jaw chucks) *VDI Standards*
[16] Byun J, Liu C 2012 Methods for improving chucking accuracy *J. of Manuf. Sci. and. Eng.* 134 (5)